Acc. Chem. Res. **1999,** *32,* 651−657

Modeling the Phase Behavior of Polymer/Clay Nanocomposites

ANNA C. BALAZS,* CHANDRALEKHA SINGH, EKATERINA ZHULINA, AND YULIA LYATSKAYA

Department of Chemical Engineering, University of Pittsburgh, Pittsburgh, Pennsylvania 15261

Received June 9, 1998

Introduction

The blending of molten polymers and inorganic clays can yield a new class of materials where nanoscale clay particles are molecularly dispersed within the polymer matrix.[1−5] Such composites exhibit dramatic increases in tensile strength and heat resistance and decreases in gas permeability when compared to the pure polymer matrix.[2] For example, adding the inorganic clay montmorillonite to nylon-6 essentially doubled the tensile strength and modulus, as well as tripled the heat distortion temperature.[2] The improvement in these properties is achieved at very low loadings of the inorganic component, namely, 1−10 wt %. Thus, the new materials are lighter in weight than conventionally filled polymers. These unique properties make the nanocomposites ideal materials for products ranging from high-barrier packaging for food and electronics to strong, heat-resistant automotive components.

Fabricating these materials in an efficient and cost-effective manner, however, poses significant synthetic challenges. To understand these challenges, it is useful to consider the structure of the clay particles. The inorganic clays (montmorillonite being a prime example) consist of stacked silicate sheets; each sheet is approximately 200 nm in length and 1 nm in thickness.[1] The spacing (or "gallery") between the closely packed sheets is also on the order of 1 nm, which is smaller than the radius of gyration of typical polymers. Consequently, there is a large entropic barrier that inhibits the polymer from penetrating this gap and becoming intermixed with the clay.

Thus, there are several critical issues that need to be addressed in order to optimize the production of these polymer/clay hybrids. Of foremost importance is isolating conditions that promote the penetration of the polymer into the narrow gallery. If, however, the sheets ultimately phase-separate from the polymer matrix, the mixture will not exhibit the improved strength, heat resistance, or barrier properties. Therefore, it is also essential to determine the factors that control the macroscopic phase behavior of the mixture. Finally, the properties of the hybrid commonly depend on the structure of the material; thus, it is of particular interest to establish the morphology of the final composite.

In this Account, we explore these issues by using computational and analytical models to probe the behavior of the nanocomposites. To date, there are few theories to pinpoint the critical parameters or predict the thermodynamic stability of the mixture,[6−8] forcing synthetic chemists to follow the inefficient Edisonian prescription of creating all possible mixtures in order to isolate the desired materials. Below, we first focus on the interactions between two closely spaced surfaces immersed in a polymer melt and determine conditions that drive the polymers into the region between the confining walls.[6] Once the sheets are separated and dispersed in the matrix, they can either display a random orientation with respect to each other or exhibit a nematic phase,[1,5] where these platelets are roughly aligned parallel to each other. To outline the "windows" of miscibility and locate the different phases, we calculate phase diagrams for the polymer/clay mixtures.[7] Finally, we present a simple kinetic argument, which we couple with our equilibrium analysis, to determine the overall morphology of the composite.[7] These findings provide useful guidelines that facilitate the fabrication of thermodynamically stable mixtures with the desired structure.

We note that the vast majority of manufactured polymeric components contain some fraction of rigid particles, or fillers.[9] Our studies of the interactions between polymers and nanoscale solids are also applicable to the commercially important class of materials referred to as filled polymers.

Polymers Penetrating the Closely Spaced Sheets

To investigate the interactions between a polymer melt and the closely spaced sheets, we use the self-consistent field (SCF) theory derived by Scheutjens and Fleer.[10] In this treatment, the phase behavior of polymer systems is modeled by combining Markov chain statistics with a mean field approximation for the free energy. The equations in this lattice model are solved numerically and self-consistently. The self-consistent potential is a function of the polymer segment density distribution and the Flory−Huggins interaction parameters, or χ values, between the different components. (Note that χ is inversely proportional to temperature; thus, variations in χ are comparable

Anna C. Balazs (born in 1953 in Budapest, Hungary) received her A.B. in physics from Bryn Mawr College in 1975 and her Ph.D. in materials science from the Massachusetts Institute of Technology in 1981. She is currently Bicentennial Engineering Alumni Faculty Fellow and Associate Professor in the Chemical Engineering Department at the University of Pittsburgh. The coauthors of this Account are Research Associates in her group.

Chandralekha Singh (born in 1964 in India) received her B.S. and M.S. in physics from the India Institute of Technology in Kharagpur in 1988 and her Ph.D. in physics from the University of California at Santa Barbara in 1993.

Ekaterina Zhulina (born in 1953 in Saratov, Russia) received her M.S. in physics from Leningrad State University in 1977 and her Ph.D. from the Institute of Macromolecular Compounds of the Russian Academy of Sciences in 1981.

Yulia Lyatskaya (born in 1966 in St. Petersburg, Russia) received her M.S. in physics from Leningrad State University in 1989 and her Ph.D. from the Institute of Macromolecular Compounds of the Russian Academy of Sciences in 1993.

10.1021/ar970336m CCC: $18.00
Published on Web 02/11/1999

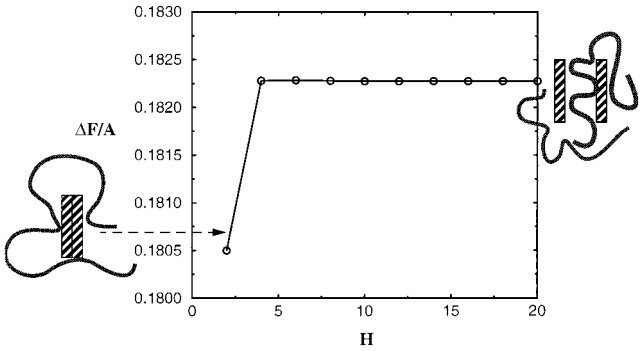

FIGURE 1. Free energy per unit area, $\Delta F/A$, versus H, for the bare surfaces in the melt. Here, $\chi_{surf} = 0$ and the polymer length is $N = 100$. The diagram on the left shows the surfaces in intimate contact, and the sketch on the right shows the polymers localized between these substrates.

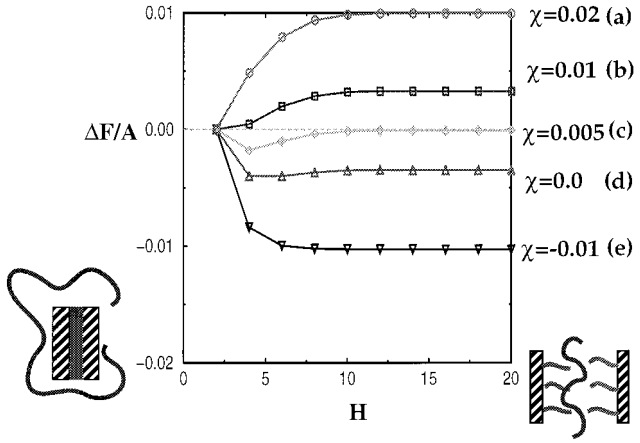

FIGURE 2. $\Delta F/A$ versus H for various χ values. The parameters are $N_{gr} = 25$, $\rho = 0.04$, $N = 100$, and $\chi_{surf} = 0$. The diagram on the left shows the reference state, where the grafted chains form a melt between the surfaces, and in the diagram on the right, the surfaces are separated by the intervening polymers.

to variations in temperature.) While such SCF calculations do not necessarily yield quantitative predictions, the results indicate how to tailor the system to modify the stability and morphology of the mixture.

Using this SCF method, we consider two infinite, parallel plates immersed in a "bath" of molten polymer. To model organically modified clays, where the sheets are coated with linear alkyl chains, we introduce terminally anchored short-chain "surfactants" onto the plates. These surfaces lie parallel to each other in the XY plane, and we investigate the effect of increasing the separation between the surfaces in the Z direction. As the surface separation is increased, polymer from the surrounding bath penetrates the gap between these walls and the calculations yield the corresponding change in the free energy, ΔF, of the system. By systematically increasing the surface separation (H), we obtain the ΔF versus H curves discussed below. In previous studies,[11] we used a similar approach to determine $\Delta F(H)$ for two polymer-coated surfaces in various solvents.

We note that the different components in these systems can contain charged species. In the following calculations, we do not consider electrostatic interactions. Nonetheless, the strong attraction between oppositely charged sites can be modeled through a large, negative value for the relevant χ. Below, we determine how the features of the surfactants, melt, and substrate affect the ability of the polymers to penetrate the gallery.[6]

Tailoring the Surfactants. To provide a basis of comparison, we first consider the behavior of the polymer melt in the presence of the bare surfaces. The interaction parameter between the polymers and the substrate is given by $\chi_{surf} = 0$, and the length of the polymers is fixed at $N = 100$ sites. In the reference state, the surfaces are in intimate contact. As the surfaces are pulled apart, polymers come in contact with the solid walls and lose conformational entropy against these impenetrable interfaces. As a result, ΔF becomes positive as H is increased (see Figure 1) and the intermixing of these components is unfavorable. In other words, at $N = 100$, the polymers and neutral sheets are immiscible and the mixture would phase-separate.

In the case of the organically modified clay surfaces, favorable enthalpic interactions between the tethered surfactants and the polymers can overwhelm the entropic losses and lead to effective intermixing of the polymer and clay. Here, the reference state (corresponding to $\Delta F = 0$) is taken to be the state where the tethered surfactants form a melt that completely saturates the space between the two walls.[12] Our aim is to isolate conditions where ΔF is reduced relative to the reference state, that is, $\Delta F < 0$. For such values, the intermixing of the polymers and modified sheets is favorable relative to the unmixed state. We first vary χ, the polymer−surfactant interaction parameter, fixing the length of the surfactants at $N_{gr} = 25$, and the grafting density at $\rho = 0.04$. (The distance between the surfactants is $1/\rho$.) Figure 2 shows the $\Delta F(H)$ profiles for various values of χ. For $\chi > 0$ (cases a and b), $\Delta F > 0$ and, consequently, the corresponding mixture would be immiscible. For $\chi \cong 0$ (cases c and d), the plots show distinct local minima for $\Delta F < 0$. Such local minima indicate that the mixture forms an "intercalated" structure.[8] In particular, the lowest free energy state is one where the polymers have penetrated the gallery and enhanced the separation between the plates by a fixed amount. For $\chi < 0$ (case e), the plot indicates that there is a global minimum at large (infinite) separations. Such plots point to an "exfoliated" structure,[8] where the sheets are effectively separated from each other and dispersed within the melt. Thus, from a purely thermodynamic argument, we see that increasing the attraction between the polymers and surfactants promotes the formation of stable composites and could result in the creation of exfoliated structures.

Increasing the length of the polymers (N) increases the disparity in the lengths of the free and grafted chains and increases the values of ΔF relative to those in Figure 2. Thus, increasing N promotes phase separation and requires more attractive χ values in order for the system to be miscible. One means of decreasing the disparity between the free and tethered chains is to increase the length of the surfactants. Figure 3 shows the free energy

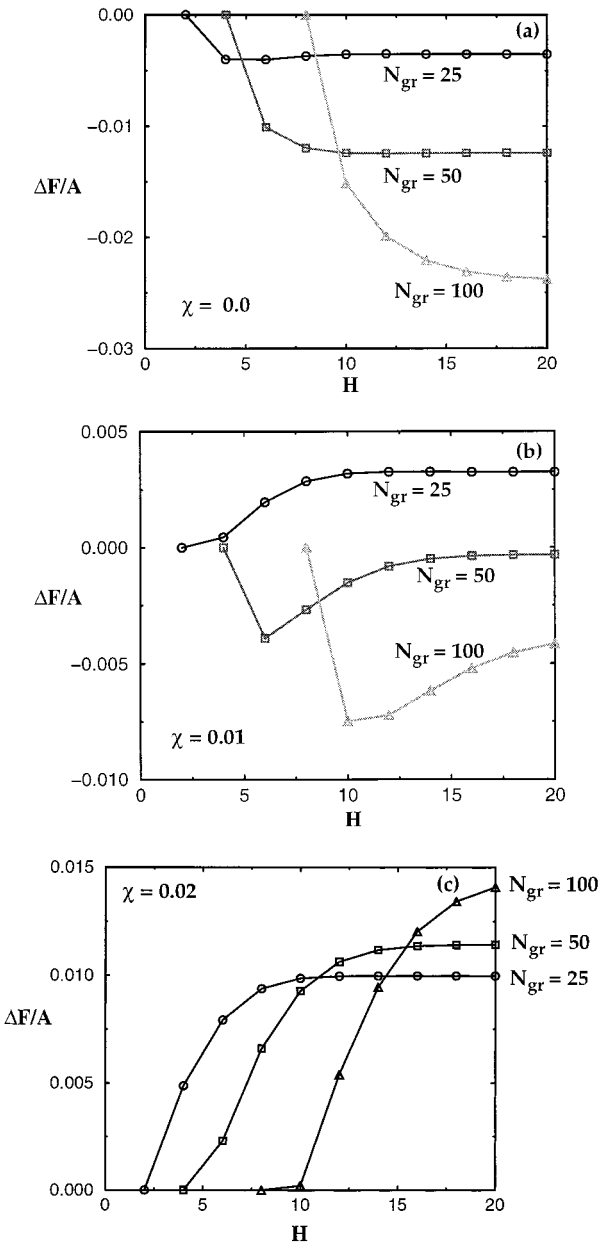

FIGURE 3. $\Delta F/A$ versus H for different surfactant lengths. Here, $\rho = 0.04$, $N = 100$, and $\chi_{surf} = 0$. The panels are for the following values of the interaction parameter: (a) $\chi = 0.0$, (b) $\chi = 0.01$, and (c) $\chi = 0.02$.

profiles[13] at various surfactant lengths (N_{gr} = 25, 50, and 100) for χ = 0, 0.01, and 0.02. The grafting density is fixed at ρ = 0.04. For the χ = 0 case, increasing the length of the tethered chain alters the structure of the composite from intercalated to exfoliated. More dramatically, for χ = 0.01, increasing N_{gr} drives an immiscible mixture to form a thermodynamically stable intercalated hybrid.

The interactions between the short surfactants and long polymers are characterized by a sharp, thin interface and little interpenetration between the different chains.[6,14] In contrast, when the polymer and surfactant are of the same length ($N_{gr} = N = 100$), the interaction between the species leads to a broad interface, or "interphase", which allows the polymers more conformational degrees of freedom

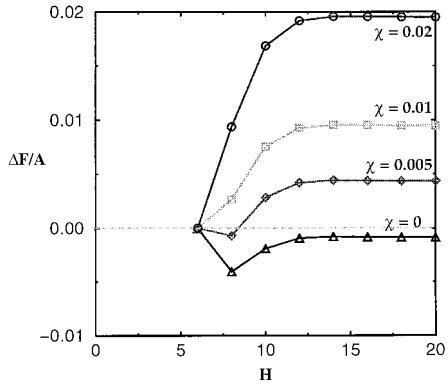

FIGURE 4. $\Delta F/A$ versus H for $\rho = 0.12$ and various χ values. Other parameters are the same as in Figure 2.

and, therefore, is more entropically favorable. As a result, the values of ΔF are lower for the longer surfactants.

Note that these entropic effects dominate even at values of χ (=0.01) where the energetic interactions are unfavorable. If, however, χ is increased beyond a critical value, energetic effects dominate and increasing the surfactant length increases the free energy. For χ = 0.02, increasing the length of the surfactant increases the number of unfavorable polymer−surfactant contacts and, thus, increases the value of ΔF. Thus, within a finite range of polymer−surfactant interactions, the miscibility and morphology of the composite can be tailored by increasing the surfactant length.

These observations agree with recent experiments on the fabrication of nanocomposites with organically modified clays and polystyrene−polybutadiene block copolymers.[15] The researchers found that increasing the length of the alkyl chains on the clay promoted insertion of the copolymer, whereas no insertion was observed with the shorter alkyl chains. The authors noted that the longer the alkyl chain, the greater the compatibility with the polystyrene block and the greater the effective strength of the material.

Finally, we note that increasing ρ to 0.12 shifts ΔF to higher values and destabilizes the mixture (see Figure 4). As the surfactant layer becomes more dense, it becomes harder for the free chains to penetrate and intermix with the tethered species. At high ρ, more attractive values of χ are needed to promote polymer penetration into the interlayer. Comparing Figures 1, 2, and 4, we see that a bare surface and a surface with too many tethered surfactants are both unfavorable for forming the hybrids. The comparison points to the fact that there is an optimal grafting density for forming polymer/clay composites.

Tailoring the Polymer Melt. In the above discussions, we considered systems where χ is varied from 0.0 to 0.02. For cases where the specified polymers are highly incompatible with the alkyl chains or underlying substrate, an alternative means of intermixing the components must be developed. The ideal scheme would be applicable to a broader range of macromolecules and would not involve the challenging task of optimizing the surfactant grafting density. Here, we introduce the notion of tailoring the melt by adding a fraction of functionalized polymers. These

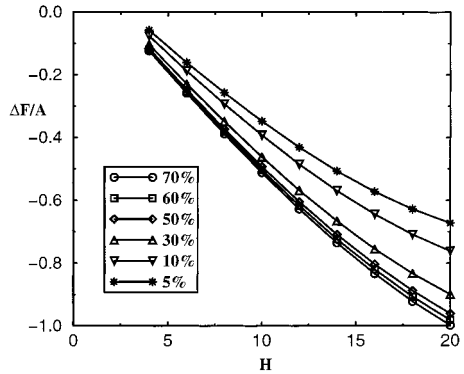

FIGURE 5. $\Delta F/A$ versus H. The melt contains two types of polymers: a functionalized chain ($N = 75$) and a slightly longer ($N = 100$) nonfunctionalized species. The functionalized polymer has a sticker at one end of the chain. The interaction between the sticker and surface is given by $\chi_{surf} = -75$. The percentages refer to the fraction of functionalized polymers. The other parameters are the same as in Figure 2.

chains contain "stickers" that are highly attracted to the surface; otherwise, they are chemically identical to the remainder of the chains in the bulk. The functionalized species will bind to the bare clay sheets and, thus, constitute long-chained surfactants. The free polymer can readily penetrate this thick grafted layer and form a broad interphase, which promotes the formation of exfoliated hybrids. While the experimental results will depend on the kinetics of the process, the SCF calculations can indicate, for example, how the fraction of functionalized chains in the mixture affects the thermodynamic stability of the product. To test the feasibility of this approach, we varied the fraction of functionalized polymers within a melt of chains of comparable length.

The functionalized polymers contain a sticker site at one end of the chain and are slightly shorter ($N = 75$) than the nonfunctionalized species ($N = 100$). (In a physical experiment, decreasing the length of the functionalized species by a small degree will permit these chains to diffuse to the surface faster than the longer chains and, once at the surface, provide an interfacial layer for the longer polymers.) The interaction between the reactive stickers and the surface[16] is characterized by $\chi_{surf} = -75$. The interaction parameter between the stickers and all other species is set equal to 0. (Thus, the stickers do not react with themselves or other monomers.) For the other monomers in the system (the nonstickers), $\chi_{surf} = 0$.

The results in Figure 5 imply that this scheme is successful in exfoliating the sheets. Note that having just a small fraction of such functionalized species in the melt promotes the dispersion of the particles. As a basis of comparison, recall that the interactions between the bare surface and nonfunctionalized polymers lead to an immiscible mixture (Figure 1). At the low-volume fraction of functionalized polymers, these chains do indeed act as high molecular weight surfactants, forming an interlayer that the polymer can readily penetrate. On the other hand, as the fraction of the functionalized chains is increased, the polymers are driven to coat the substrates and, consequently, the surfaces are pushed apart by the

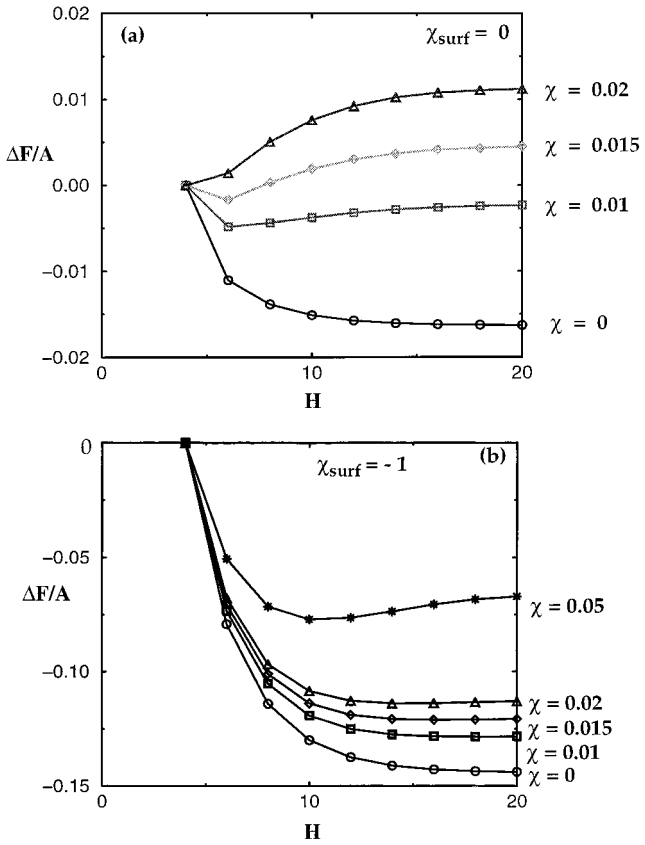

FIGURE 6. $\Delta F/A$ versus H in the presence of polymer−surface interactions. The other parameters are $N = 100$, $N_{gr} = 100$, and $\rho = 0.02$. The values of the polymer−surface interaction are (a) $\chi_{surf} = 0$ and (b) $\chi_{surf} = -1$.

adsorbing chains. Note that increasing the fraction of functionalized chains beyond 30% has little effect on decreasing ΔF. In effect, once the surfaces have been coated with the "sticky" polymers, increasing the volume fraction of these species does not lead to further decreases in this free energy. For that matter, since all curves in Figure 5 point to an exfoliated system, the most cost-effective treatment could be the 5% example, where only a small fraction of functionalized species is required for the process.

The above results point to another route for forming stable polymer/clay dispersions. Instead of the functionalized polymers, a small fraction of AB diblock copolymers could be added to a melt of B polymers or a melt composed entirely of AB diblocks could be employed. Here, a short hydrophilic A block will anchor the chain to the bare (nonmodified) clay sheets. The large organophilic B block will extend away from the surface, and could drive the separation and dispersion of these sheets.

Tailoring the Substrate. The plots in Figure 6 show the effect of introducing a relatively large attraction ($\chi_{surf} = -1$) between the polymers and the underlying substrate. By comparing parts a and b of Figure 6, we see that a highly attractive surface interaction could promote the formation of exfoliated composites from previously intercalated structures or immiscible components. Even when the interaction between the polymer and surfactants is relatively unfavorable ($\chi = 0.05$), the presence of the

attractive substrate drives the system to form an intercalated hybrid. As indicated above, the effect of a large, negative χ_{surf} is comparable to the effect of a strong electrostatic attraction between the polymer and surface. Thus, the equilibrium results indicate that tailoring the relative charge or polarity of the substrate provides a means of controlling the phase behavior and structure of the mixture. As we caution below, the kinetics of polymer interpenetration can, however, lead to trapped states that affect the morphology of the final hybrid.

Having isolated conditions that promote the dispersion of these particles within the matrix, we now turn our attention to determining the phase diagram for the mixture. For this calculation, we must utilize a more macroscopic model than the SCF; we describe the model below. We now assume that the sheets are well-separated and can undergo random mixing with the homopolymers (polymers that contain only one type of monomer). We first determine the factors that affect the miscibility of these two components and then formulate a simple kinetic argument to establish the morphology of the final composite.[7]

Modeling the Macroscopic Phase Behavior of the Polymer/Clay Mixture

The Model. The actual sheets are roughly oblong in shape and possess a very high aspect ratio, being approximately 200 nm in diameter and 1 nm in width. To capture this physical asymmetry, we model the individual particles as broad, rigid disks of diameter D and thickness L. The homopolymers are modeled as flexible chains of length N. The volume fraction of disks in the incompressible blend is ϕ_d, and $\phi_p = 1 - \phi_d$ is the volume fraction of polymer. The interaction between a monomeric unit in the polymer chain and a surface site on the disk is characterized by the Flory–Huggins interaction parameter, χ.

In the mixed state, the broad disks can be either randomly oriented with respect to each other and form an isotropic phase or relatively aligned and form a nematic phase. A nematic ordering is especially beneficial in decreasing the permeability of gases through polymer/clay films.[1] To analyze the miscibility of the homopolymer/disk mixture and investigate the formation of the isotropic and nematic structures, we modify the Onsager model[17–19] for the nematic ordering of rigid rods. The free energy of the mixture has the following form:[7]

$$F = F_{conf} + F_{ster} + F_{int} + F_{transl} \qquad (1)$$

The term F_{conf} describes the conformational losses due to the alignment of the disks, F_{ster} accounts for the steric interactions between the disks, F_{int} describes the enthalpic contributions due to polymer–disk contacts, and F_{transl} takes into account the translational entropy of disks. Using this approach, we obtain the following expression for the free energy:[10]

$$F = n_d(\text{constant} + \ln \phi_d + \sigma - \ln(1 - \phi_d)(b/v_d)(\rho - 1) - \chi v_d \phi_d) + n_p \ln \phi_p \qquad (2)$$

where n_p is the number of polymer molecules, n_d is the number of disks per unit volume, and $v_d = (\pi D^2 L)/4$ is the volume of an individual disk. The parameters σ and ρ allow us to distinguish between the isotropic and nematic phases; σ effectively describes the orientation of the disks with respect to the nematic direction and $\rho = (4/\pi)\langle|\sin \gamma|\rangle$, where γ is the angle between two disks. In the isotropic phase, $\sigma = 0$ and $\rho = 1$, while in the nematic phase, $\sigma_n = 2 \ln(-(2/\sqrt{\pi})(v_d/b) \ln(1 - \phi_d)) - 1$ and $\rho_n = -2(v_d/b)/\ln(1 - \phi_d)$.

To construct the equilibrium phase diagram, we equate the chemical potentials of the disks and polymer in the isotropic and nematic phases: $\mu^i_d = \mu^n_d$, $\mu^i_p = \mu^n_p$, where $\mu^i_k = (\delta F_i)/(\delta n_k)|_{n_{j\neq k}=\text{const}}$. We solve this system of equations numerically and present the results as plots that highlight the role of χ, ϕ_d, and N in the phase behavior of the system.

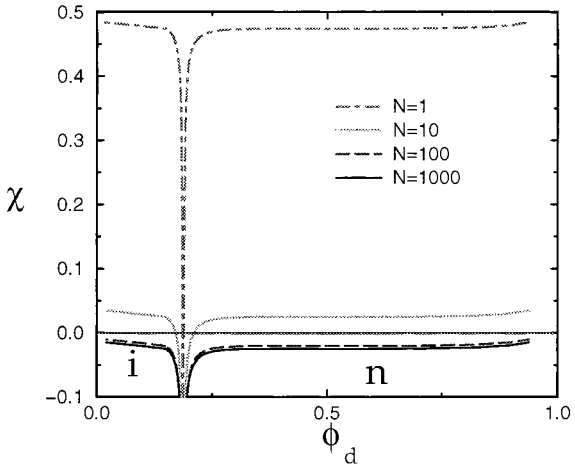

FIGURE 7. Phase diagrams for disks and polymers of various N values plotted as a function of χ vs ϕ_d, where ϕ_d is the volume fraction of the disks. The diameter of the disks is $D = 30$, and their width is $L = 1$. The area above the phase boundaries encompasses the region of immiscibility. The miscible regions lie below the boundaries. Within the regions of miscibility, i marks the isotropic phase and n indicates the nematic phase. The plots reveal that increasing N increases the region of immiscibility.

Analyzing the Phase Behavior and Morphology of the Mixture. Figure 7 shows the phase diagrams for the polymer/disk mixtures in the χ versus ϕ_d coordinate frame for various homopolymer lengths, N. The diameter of the disks is fixed at $D = 30$, and the width L is set at 1. The solid curves mark the phase boundaries for the system. The area between the respective boundaries encompasses the phase-separated region. The two regions below the boundaries pinpoint the regions of miscibility: the mixture forms an isotropic phase (i) at low concentrations of disks and exhibits a nematic phase (n) at high ϕ_d.

As can be seen from the figure, the region of miscibility decreases with an increase in N. The plots further reveal that, for relatively high N ($N \geq 100$), phase separation occurs even at negative values of χ, where there is an

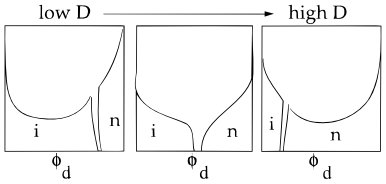

FIGURE 8. Schematic phase diagrams illustrating the effect of increasing the disk diameter.

attractive interaction between the two components. In other words, at $N \geq 100$, the polymer and disks are totally immiscible even if there is no repulsion between these components, indicating an entropically driven phase separation. Note that this result agrees with our finding from the SCF calculations; Figure 2 shows that, for $N = 100$, the polymer and bare surface are immiscible even at $\chi_{surf} = 0$. The SCF results also show that increasing N promotes phase separation between the sheets and polymer.

The analytical model also indicates the effect of varying the size of the clay sheets. In particular, increasing the diameter of the disks promotes the nematic ordering of disks at lower values of ϕ_d. This behavior is illustrated schematically in Figure 8. Note that in the two limiting cases of low and high D, there is the possibility of isotropic−isotropic (i−i) phase coexistence in the former case and nematic−nematic (n−n) phase coexistence in the latter case. Our main interest is in the isotropic−nematic transition; thus, we do not consider instances of i−i and n−n coexistence.

As mentioned at the beginning of this equilibrium analysis, the disks are assumed to be well-separated from each other. Thus, each particle could undergo random mixing with the polymer. In reality, however, this situation might not be reached. Consider the mixing of the polymer and clay agglomerate;[5] within the agglomerate, the individual crytallites or sheets are arranged in the closely spaced parallel stacks. In order for the different components to intermix, the polymer must penetrate the gap from an outer edge and then diffuse toward the center of the gallery. When the polymer moves through the gap, two scenarios are possible, depending on the value of χ. In the first case, $\chi \geq 0$ and there is no attraction between the polymer and disks. Here, the polymer can separate the disks, as the chain tries to retain its coillike conformation and gain entropy. In the second case, $\chi < 0$ and the polymer and disks experience an attractive interaction. Here, the polymer "slides" through the gallery, maximizing contact with the two confining surfaces. The overall conformation of the polymer is rather "flat", but the losses in conformational entropy are compensated by enthalpic gains when the chain comes in contact with one of the disks. The final morphology of the mixture will obviously be different for the two scenarios. In the first case, the disks will be totally separated and dispersed in the polymer matrix, forming an exfoliated structure. In the second case, the disks are effectively glued together by the intervening polymer and the platelets remain parallel to each other, forming an intercalated structure.

We can now combine the results of the equilibrium study with our kinetic arguments to analyze the structure of the final composite. As discussed above, a true exfoliated structure, where the disks are totally separated, can only occur for $\chi \geq 0$. The equilibrium analysis, however, shows that for $\chi \geq 0$, the homopolymers and disks will ultimately demix *unless* the polymer is relatively short, namely, $N < 100$. Therefore, a stable exfoliated structure can only be attained by mixing disks with relatively short homopolymers.

Again from kinetic considerations, we observed that an intercalated structure is expected when $\chi < 0$. The equilibrium analysis (see Figure 7) shows that χ must be negative for mixtures of long homopolymers and disks to be thermodynamically stable. Combining these arguments, we see that stable mixtures of high molecular weight polymers and discotic particles will exhibit an intercalated morphology.

More systematic experimental studies are needed to test our prediction on the role of χ and N in determining the morphology of the mixture. Nonetheless, recent experiments on mixtures of clays and high molecular weight styrene-derivative polymers[20] show qualitative agreement with our results. Here, the derivatized polymers are polar in nature and readily interact with polar moieties on the surface of the clay; in other words, the interaction between the polymers and clay is relatively attractive. The molecular weights of the chains were at least $M_w = 30\,000$ ($\approx N > 300$). As anticipated from our discussion above, all the samples exhibited an intercalated structure. Furthermore, when long, nonpolar polymers (which are not attracted to the surface of the clays) were employed in the process, the mixture was immiscible.

Conclusions

We used two distinct theoretical methods to probe the interactions between polymers and clay sheets or, more generally, solid particles. Through the SCF models, we determined the free energy profiles as a polymer melt penetrates the gap between bare and organically modified sheets. The shapes of the profiles reveal whether the polymer−clay interaction is favorable and, thus, if the mixture is miscible. For miscible mixtures, the curves indicate the morphologies (intercalated vs exfoliated) of the composite. Through these calculations, we could modify the characteristics of the surfactants, polymers, and substrate and thus isolate factors that drive the polymers to permeate the clay galleries. This model will not, however, yield a complete phase diagram for the system.

To generate such a phase diagram, we developed an Onsager-type theory for a mixture of homopolymers and rigid disks. Through this model, we could take into account the possible nematic ordering of the disks and pinpoint the boundaries for the isotropic, nematic, and phase-separated regions of phase space. Both this macroscopic approach and the more mesoscopic SCF calculations show that the favorable mixing of the polymer and disks is controlled through a balance of the effects of N and χ. In particular, an increase in N requires a decrease in χ for the mixture to be thermodynamically stable.

As we noted above, the actual phase behavior and morphology of the mixture can be affected by the kinetics

of the polymers penetrating the gap. Combining the results of our equilibrium studies with simple kinetic arguments, we predict that, for large N and $\chi < 0$, a stable hybrid will only exhibit an intercalated morphology. Recent experimental studies[20] reveal that the melt mixing of organically modified clays and highly attractive polymers does in fact lead to intercalated hybrids.

The above results provide design criteria for synthesizing optimal exfoliating agents. For facile penetration into the gallery, the polymer must contain a fragment that is highly attracted to the surface. This fragment also promotes miscibility between the polymer and clay.[21] In addition, this copolymer must contain a longer fragment that is not attracted to the sheets. The nonreactive block will attempt to gain entropy by pushing the sheets apart. Once the sheets are separated, these blocks will also sterically hinder the surfaces from coming into close contact. Our SCF results on melts containing functionalized polymers give credence to this scheme. These results also reveal that the optimal polymeric candidates for creating stable exfoliated composites are those that would constitute optimal steric stabilizers for colloidal suspensions.

Finally, we note that our findings are also relevant to the behavior of fiber-reinforced composites. Here, our substrate represents the surface of a fiber and the "surfactants" represent a coating, which is applied to enhance the adhesion between the fiber and polymer matrix. The spacing between the fibers in such materials is sufficiently large that the dynamic aspects of the fiber−matrix interaction will not necessarily lead to kinetically trapped states. Thus, the equilibrium results that point to thermodynamically stable hybrids are useful in indicating ways of tailoring the interphase and improving the adhesion between the fibers and polymers within the composite.

We gratefully acknowledge support from the Army Office of Research, the Office of Naval Research, and the National Science Foundation.

References

(1) Yano, K.; Uzuki, A.; Okada, A.; Kurauchi, T.; Kamigaito, O. Synthesis and Properties of Polyimide-Clay Hybrid. *J. Polym. Sci., Part A: Polym. Chem.* **1993**, *31*, 2493−2498.

(2) Kojima, Y.; Usuki, A.; Kawasumi, M.; Okada, A.; Kurauchi, T.; Kamigaito, O. J. Synthesis of Nylon 6-Clay Hybrid by Montmorillonite Intercalated with ϵ- Caprolactam. *Polym. Sci., Part A: Polym. Chem.* **1993**, *31*, 983−986.

(3) Vaia, R. A.; Jandt, K. D.; Kramer, E. J.; Giannelis, E. P. Kinetics of Polymer Melt Intercalation. *Macromolecules* **1995,** *28*, 8080−8085.

(4) Messersmith, P. B.; Stupp, S. I. Synthesis of Nanocomposites: Organoceramics. *J. Mater. Res.* **1992**, *7*, 2599−2611.

(5) Krishnamoorti, R.; Vaia, R. A.; Giannelis, E. P. Structure and Dynamics of Polymer- Layered Silicate Nanocomposites. *Chem. Mater.* **1996**, *8*, 1728−1734.

(6) Balazs, A. C.; Singh, C.; Zhulina, E. Modeling the Interactions Between Polymers and Clay Surfaces Through Self-consistent Field Theory. *Macromolecules* **1998**, *31*, 8370−8381.

(7) Lyatskaya, Y.; Balazs, A. C. Modeling the Phase Behavior of Polymer-Clay Composites. *Macromolecules* **1998**, *31*, 6676−6680.

(8) Vaia, R. A., Giannelis, E. P. Lattice Model of Polymer Melt Intercalation in Organically-Modified Layered Silicates. *Macromolecules* **1997,** *30*, 7990−7999.

(9) Utracki, L. A. *Polymer Alloys and Blends*; Hanser Publishers: Munich, 1989.

(10) Fleer, G.; Cohen-Stuart, M. A.; Scheutjens, J. M. H. M.; Cosgrove, T. Vincent, B. *Polymers at Interfaces*; Chapman and Hall: London, 1993.

(11) Singh, C.; Pickett, G.; Zhulina, E. B.; Balazs, A. C. Modeling the Interactions Between Polymer-Coated Surfaces. *J. Phys. Chem., B* **1997**, *101*, 10614−10624.

(12) Our SCF calculations are based on an incompressible model. In the reference state for the organically modified clays, we consider the system to be composed of the two surfaces and the tethered surfactants; there are no void or solvent sites in the system.

(13) In the reference state, the surfactants form a melt that completely fills the gap between the surfaces. Since the length of the surfactants is now being varied, the reference states for different values of N_{gr} (= 25, 50, 100) are not identical. Namely, the shorter chains will achieve this state at smaller surface separations than the longer surfactants.

(14) Leibler, L.; Mourran, A. Wetting on Grafted Polymer Films. *Mater. Res. Soc. Bull.* **1997**, *22*, 33−37.

(15) Laus, M.; Francescangeli, O.; Sandrolini, F. New hybrid nanocomposites based on organophilic clay and poly(styrene-b-butadiene) copolymers. *J. Mater. Res.* **1997**, *12*, 3134−3139.

(16) In the case of surface adsorption, we must divide χ_{surf} by the coordination number of the cubic lattice in order to relate this Flory−Huggins parameter to experimentally relevant values. Thus, our value of χ_{surf} is comparable to a binding energy of (75/6) = 12.5 kT.

(17) Onsager, L. The Effects of Shape on the Interaction of Colloidal Particles. *Ann. N. Y. Acad. Sci.* **1949**, *51*, 627−659.

(18) Odijk, T. Theory of Lyotropic Polymer Liquid Crystals. *Macromolecules* **1986**, *19*, 2313−2329.

(19) (a) Khokhlov, A. R., Semenov, A. N. On the Theory of Liquid-Crystalline Ordering of Polymer Chains with Limited Flexibility. *J. Stat. Phys.* **1985**, *38*, 161−182. (b) Khokhlov, A. R., Semenov, A. N. Theory of Nematic Ordering in the Melts of Macromolecules with Different Flexibility Mechanisms. *Macromolecules* **1986**, *19*, 373−378.

(20) Vaia, R. A., Giannelis, E. P. Polymer Melt Intercalation in Organically-Modified Layered Silicates: Model Predictions and Experiment. *Macromolecules* **1997**, *30*, 8000−8009.

(21) Note that the thick adsorbed layer of end-functionalized chains effectively decreases the aspect ratio, D, of the disk. As can be seen from Figure 8, decreasing D increases the region of miscibility for the isotropic phase. In this way, adsorbed, end-functionalized chains promote the thermodynamic stability of the homogeneous mixture.

AR970336M